Received: 8 June 2021 | Revised: 22 September 2021 | Accepted: 24 October 2021

DOI: 10.1111/cas.15181

ORIGINAL ARTICLE

Cancer Science WILEY

# Identification of *RET* fusions in a Chinese multicancer retrospective analysis by next-generation sequencing

Minke Shi[1] | Weiran Wang[2] | Jinku Zhang[3] | Bobo Li[4] | Dongxiao Lv[5] | Danhua Wang[2] | Sizhen Wang[6] | Dezhi Cheng[7] | Tonghui Ma[2]

[1]Department of Thoracic and Cardiovascular Surgery, The Affiliated Drum Tower Hospital of Nanjing University Medical School, Nanjing, China

[2]Department of Translational Medicine, Genetron Health (Beijing) Technology, Co. Ltd., Beijing, China

[3]Department of Pathology, Key Laboratory of Molecular Pathology and Early Diagnosis of Tumor in Hebei Province, The First Centre Hospital of Baoding, Baoding, China

[4]Department of Thoracic Surgery, Shandong Cancer Hospital Affiliated to Shandong University, Jinan, China

[5]Tumor Research and Therapy Center, Shandong Provincial Hospital Affiliated to Shandong First Medical University, Jinan, China

[6]Genetron Health (Beijing) Technology, Co. Ltd., Beijing, China

[7]Department of Thoracic Surgery, The First Affiliated Hospital of Wenzhou Medical University, Wenzhou, China

**Correspondence**
Dezhi Cheng, Department of Thoracic Surgery, The First Affiliated Hospital of Wenzhou Medical University, Southern White Elephant Town, Ouhai District, Wenzhou, Zhejiang 325000, China.
Email: dezhicheng@sina.com

Tonghui Ma, Department of Translational Medicine, Genetron Health (Beijing) Co. Ltd, Building 11, Zone 1, 8 Life Science Parkway, Beijing 102200, China.
Email: tonghuima@yeah.net

Funding information
The paper was supported by grants from the Wenzhou Municipal Science and Technology Bureau of China (No. Y20180175)

## Abstract

Fusion of *RET* with different partner genes has been detected in papillary thyroid, lung, colorectal, pancreatic, and breast cancer. Approval of selpercatinib for treatment of lung and thyroid cancer with *RET* gene mutations or fusions calls for studies to explore *RET* fusion partners and their eligibility for RET-based targeted therapy. In this study, *RET* fusion patterns in a large group of Chinese cancer patients covering several cancer types were identified using next-generation sequencing. A total of 44 fusion patterns were identified in the study cohort with *KIF5B*, *CCDC6*, and *ERC1* being the most common *RET* fusion partners. Notably, 17 novel fusions were first reported in this study. Prevalence of functional *RET* fusions was 1.05% in lung cancer, 6.03% in thyroid cancer, 0.39% in colorectal cancer, and less than 0.1% in gastric cancer and hepatocellular carcinoma. Analysis showed a preference for fusion partners in different tumor types, with *KIF5B* being the common type in lung cancer, *CCDC6* in thyroid cancer, and *NCOA4* in colorectal cancer. Co-occurrence of *EGFR* mutations and *RET* fusions with rare partner genes (rather than *KIF5B*) in lung cancer patients was correlated with epidermal growth factor receptor-tyrosine kinase inhibitor resistance and could predict response to targeted therapies. Findings from this study provide a guide to clinicians in determining tumors with specific fusion patterns as candidates for RET targeted therapies.

**Abbreviations:** cfDNA, cell-free DNA; CRC, colorectal cancer; FFPE, formalin-fixed paraffin-embedded; GC, gastric cancer; HCC, hepatocellular carcinoma; IHC, immunohistochemistry; LC, lung cancer; NGS, next-generation sequencing; NSCLC, non-small-cell lung cancer; PTC, papillary thyroid cancer; RET, rearranged during transfection; TKI, tyrosine kinase inhibitor.

Minke Shi, Weiran Wang, and Jinku Zhang contributed equally to this work.

KEYWORDS

EGFR-TKI resistance, lung cancer, multicancer, NGS, *RET* fusion

## 1 | INTRODUCTION

*RET* was initially discovered as a rearranged oncogene in a 3T3 fibroblast cell line transfected with a human lymphoma DNA.[1] The *RET* gene encodes a receptor-tyrosine kinase, which plays an important role in cell proliferation, migration, and differentiation.[2-5] *RET* fusion induces oncogenic activation and occurs in approximately 5%-10% of sporadic PTC types and in 1%-2% of lung cancer cases with low frequency in other solid cancer types (breast cancer, <0.21%. colorectal cancer, <0.26%. esophageal cancer, <0.17%. ovarian cancer, <0.17%. prostate cancer, <0.08% and stomach cancer, <0.81%).[6-8,9-13,14-16] In tumors with activating *RET* fusions, a 5′-terminal partner gene coding sequence is fused to 3′-terminal *RET* kinase domain coding sequence including the kinase domain (NM_020975: exons 12-18).[17,18]

The most common breakpoints in *RET* occur in intron 11, followed by intron 10.[19] Multiple N-terminal partner genes of *RET* fusion have been identified. In PTCs, the most common *RET* fusions include *CCDC6-RET* (RET/PTC1) and *NCOA4-RET* (RET/PTC3), which are detected in approximately 90% of *RET* fusion-positive cases.[8,20] The most common *RET* fusions in NSCLC are *KIF5B-RET*, *NCOA4-RET*, and *CCDC6-RET*.[21,22] Multiple rare *RET* fusions have been discovered and reported in different cancers.[23,24,25-27,28,29-31]

Selpercatinib (LOXO-292) was approved by the US FDA for treatment of NSCLC, thyroid cancer, and medullary thyroid cancer with *RET* mutations or fusions.[32] In addition, it has shown effectiveness in other solid cancer types including brain cancer and pancreatic cancer.[33-35] Various molecular testing methods have been developed for detection of *RET* fusions, including NGS, RT-PCR, FISH, and IHC. Immunohistochemistry is limited for general application due to its low sensitivity and specificity.[13,36,37] Reverse transcription-PCR can only detect *RET* fusions with known fusion partners.[29,38,39] Although FISH is highly sensitive, it requires special technical expertise and is not effective for identification of fusion partners.[38,40] The NGS platform provides a more feasible way for comprehensive and accurate diagnostic testing of *RET* fusion for cancer patients who could benefit from RET inhibitors. In addition, it can be used to identify other genetic alterations.

In this study, 12 888 LC patients, 2848 CRC patients, 1785 HCC patients, 1169 GC patients, and 232 PTC patients from China were retrospectively analyzed for *RET* fusion using NGS. A total of 164 functional *RET* fusions and 58 nonfunctional fusions were identified. Notably, 17 of the 164 functional *RET* fusions were novel. Identification of these genomic fusion patterns will facilitate rationalization of clinical treatment strategies.

## 2 | MATERIALS AND METHODS

### 2.1 | Patients and samples

Tumor samples (tissues or plasma fractions) obtained from patients between January 2017 and December 2019 were used for NGS *RET* fusion detection (Genetron Health).

### 2.2 | DNA sequencing

DNA samples from LC, CRC, HCC, and GC patients were analyzed using targeted deep sequencing using NGS technology. Genomic DNA was extracted from FFPE samples using QIAamp DNA FFPE tissue kit (Qiagen) following the manufacturer's instructions. Plasma cfDNA was extracted using MagMAX Cell Free DNA Isolation Kit (Thermo Fisher Scientific). DNA samples were quantified with the Qubit 2.0 Fluorometer using Qubit dsDNA HS Assay kit (Life Technologies) following the manufacturer's instructions. Genomic DNA from each FFPE sample was sheared into 150-200-bp fragments using the M220 Focused-ultrasonicator (Covaris). Fragmented genomic DNA and cfDNA libraries were constructed with the KAPA HTP Library Preparation Kit (KAPA Biosystems) following the manufacturer's protocol. Concentration of DNA in the library was determined using the Qubit dsDNA HS Assay kit. DNA libraries were analyzed using Onco PanScan (Genetron Health), which is an 825-gene panel including major tumor-related genes. Quality control was undertaken on raw sequencing data to remove adapters and low-quality regions using Trimmomatic (version 0.36). Local alignments of reads to the hg19 genome (GRch37) were carried out using the Burrows-Wheeler Aligner tool (version 0.7.10).[41] Somatic single-nucleotide variants were retrieved using muTect (https://software.broadinstitute.org/cancer/cga/mutect),[42] somatic insertions and deletions were retrieved using Strelka (https://github.com/Illumina/strelka),[43] and structural variations were determined using GeneFuse version 0.6.1 (https://github.com/OpenGene/GeneFuse).[44] A total of 1000 genomes and variants with population frequency over 0.1% were excluded based on guidelines by the Exome Aggregation Consortium. The other variants were annotated with Oncotator and Vep.

### 2.3 | Papillary thyroid cancer sample sequencing

DNA and RNA extracted from PTC samples were analyzed with the FSZ-Thyroid-V1 NGS Panel using one-step multiplex PCR targeted amplicons as described previously.[45] DNA and total RNA

were isolated from FNA samples using AllPrep DNA/RNA Mini Kit (Qiagen) according to the manufacturer's instructions. DNA and RNA concentrations were determined using a Qubit 3.0 Fluorometer (Thermo Fisher Scientific). Ten nanograms of RNA was reverse transcribed into cDNA using SuperScript III Reverse Transcriptase (Thermo Fisher Scientific). Libraries were prepared from 10 ng DNA and 10 ng cDNA and normalized for template preparation, on the Ion Chef System (Thermo Fisher Scientific). The libraries were sequenced on the Ion Proton (Thermo Fisher Scientific) platform following the manufacturer's protocol. Data analysis and interpretation were carried out using Torrent Suite (version 5.2.2; Thermo Fisher Scientific).

### 2.4 | RNA sequencing

A 395-gene RNA panel was analyzed to identify gene fusions at the transcript level. Total RNA was isolated using the AllPrep DNA/RNA Mini Kit (Qiagen), then reverse transcribed to cDNA using SuperScript III Reverse Transcriptase (Thermo Fisher Scientific). The libraries were constructed with the KAPA HTP Library Preparation Kit (KAPA Biosystems). DNA libraries were captured with an Agilent SureSelect V5 system (Agilent) and the captured samples were subjected to Illumina HiSeq X-Ten for paired end sequencing. Sequencing reads were mapped to a human reference genome (hg19) using Hisat2-2.0.5.[46] Gene fusions were identified using FusionMap.[47]

### 2.5 | Statistical analyses

Categorical variables were compared using Pearson's analysis and $\chi^2$ test. Analyses and data presentation were undertaken using GraphPad Prism (8.0.1) and R (version 4.1.1).

## 3 | RESULTS

### 3.1 | Patient characteristics

Functional *RET* fusions occur when the *RET* gene is located in the 3′-terminal with final transcripts containing *RET* kinase domain (exons 12-18).[40,45,48] This fusion can generate a constitutively active chimeric protein with an N-terminal kinase domain characteristic of RET protein. A total of 222 *RET* fusions in 185 patients were identified using this criterion, including 164 functional fusions and 58 nonfunctional fusions (Tables S1 and S2, Figure 1A). Most of the functional fusions identified in this study have been reported previously; however, 17 functional fusions were identified for the first time. Analysis of all samples (12 888 LC patients, 2848 CRC patients, 1785 HCC patients, 1169 GC patients, and 232 PTC patients) showed that 162 (0.86%) patients harbored functional *RET* fusions with 1.05% (135/12888) in the LC group, 0.39% (11/2848) in the CRC group, 0.06% (1/1785) in the HCC group, 0.09% (1/1169) in the GC group, and 6.03% (14/232) of PTC patients (Figure 1B). Analysis of the 135 *RET* fusion-positive LC patients showed that 55 (40.74%) of them were men and 80 (59.26%) were women. The fusions occurred more frequently in younger patients ($P < .001$), women ($P < .001$), and patients with adenocarcinoma ($P < .001$). Analysis of patients in the CRC and PTC cohorts showed no preference pattern in terms of gender or age in the *RET* fusion-positive cohort. However, there was significant difference ($P = .002$) in *RET* fusion-positive rates between colon and rectum cancers (Table 1).

### 3.2 | Identification of *RET* fusion partners in patients with different cancer types

Analysis of the functional *RET* fusions in LC showed that the most common partner genes were *KIF5B*, with 85 *KIF5B-RET* fusion events identified (62.04%). The second and third most frequent fusion partners were *CCDC6* and *ERC1* (21.17%, 29/137 and 2.19%, 3/137, respectively) (Figure 2A). Several rare and novel *RET* fusion partners were identified in this study, including *DNER*, *DPP6*, *FGD5*, *GADL1*, *GLI3*, *GPRC6A*, *IL1RAPL2*, *KIAA1598*, *KIF13A*, *MALRD1*, *SPECC1*, *TLN1*, and *ZNF33B* (Table 2). In addition, multiple *RET* fusions were identified in one individual patient (such as *KIF5B-RET* and *GLI3-RET* identified in one patient, *KIF5B-RET* and *MALRD1-RET* in another patient).

In addition to lung cancer and papillary thyroid carcinoma, *RET* fusions have been found in 0.6%-0.7% of patients with other types of cancer, including breast, colon, esophageal, ovarian, prostate, and stomach cancers.[6-8,9-13,14-16] In this study, 2848 CRC patients, 1785 HCC patients, 1169 GC patients, and 232 PTC patients were retrospectively analyzed. The findings showed that 27 patients had functional *RET* fusions (11 with CRC; 1 with HCC, 1 with GC, and 14 with PTC) (Table 2). Common fusion partner genes in these groups

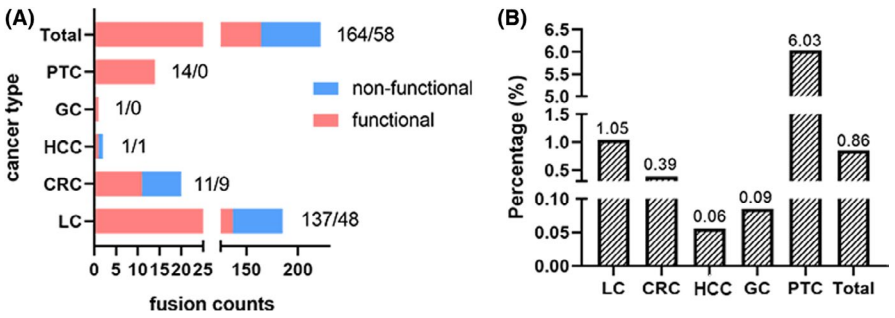


FIGURE 1 *RET* fusions identified in different cancers. A, Counts of functional and nonfunctional *RET* fusions identified in different cancer types. B, Proportion of functional *RET* fusions identified in different cancer types. CRC, colorectal cancer; GC, gastric cancer; HCC, hepatocellular carcinoma; LC, lung cancer; PTC, papillary thyroid cancer

**TABLE 1** Relationships between *RET* fusion and clinicopathologic features in cancer patients

| | | | *RET* fusion | | *P* value |
|---|---|---|---|---|---|
| | **Feature** | **Total** | **Positive** | **Negative** | |
| Lung cancer | Age, y | | | | |
| | Mean | 62.9 | 55.6 | 62.9 | <.001 |
| | Median | 63 | 57 | 64 | |
| | Range | 17-101 | 23-92 | 17-101 | |
| | Sex | | | | |
| | Male | 7211 | 55 | 7156 | <.001 |
| | Female | 5677 | 80 | 5597 | |
| | Histotype | | | | |
| | ADC | 7991 | 102 | 7889 | <.001 |
| | Non-ADC | 1169 | 1 | 1168 | |
| | Unknown | 3728 | 32 | 3696 | |
| Colorectal cancer | Age, y | | | | |
| | Mean | 59.1 | 65.8 | 59.1 | .062 |
| | Median | 61 | 62 | 61 | |
| | Range | 18-94 | 52-83 | 18-94 | |
| | Sex | | | | |
| | Male | 1744 | 9 | 1735 | .274 |
| | Female | 1104 | 2 | 1102 | |
| | Tumor location | | | | |
| | Colon | 1449 | 11 | 1438 | .002 |
| | Rectum | 1223 | 0 | 1223 | |
| | Unknown | 176 | 0 | 176 | |
| Thyroid cancer | Age, y | | | | |
| | Mean | 44.0 | 38.7 | 44.4 | .092 |
| | Median | 45 | 37 | 45 | |
| | Range | 13-75 | 25-57 | 13-75 | |
| | Sex | | | | |
| | Male | 63 | 2 | 61 | .420 |
| | Female | 169 | 12 | 157 | |
| | Histotype | | | | |
| | PTC | 232 | 14 | 218 | |

Abbreviations: ADC, adenocarcinoma; PTC, papillary thyroid cancer.

were *NCOA4* and *CCDC6*, whereas no *KIF5B-RET* fusion was identified in this group of samples (Figure 2B,C). Notably, the common partner genes were different in different cancers, implying that the hotspots of chromosome breakpoints in the partner genes are different, which might be associated with difference in sensitivity to RET inhibitors.

### 3.3 | Genomic breakpoints in *RET* of patients with different cancer types

Fusion-mediated *RET* activation is induced by different mechanisms, including increased kinase expression due to replacement of the 5′-upstream *RET* promoter with that of fusion partners,[7,49] and dimerization/oligomerization of the *RET* kinase domain mediated by a C-terminal domain present in the fusion partners that leads to ligand-independent kinase activation.[40,45,48,50] Breakpoints in *RET* and its fusion partners mainly occur in the intronic regions, therefore, the ORF is retained after mRNA splicing. A *RET* in intron 11, the most common breakpoint in LC patients, allowed exon 12 to be retained in the fusion product. In addition, breakpoints in introns 7, 8, 9, and 10 of *RET* were observed in this study (Figure 3). Notably, breakpoints in intron 11 were the most common types in these malignancies, and breakpoints in intron 8, 9, and 10 were also observed (Figure 3). The functional *RET* fusion might result in oncogenic activation due to the remaining intact *RET* kinase domain (Figure 4). Various upstream 5′ gene partners contribute different domains, typically coiled-coil domains, to RET fusion proteins and

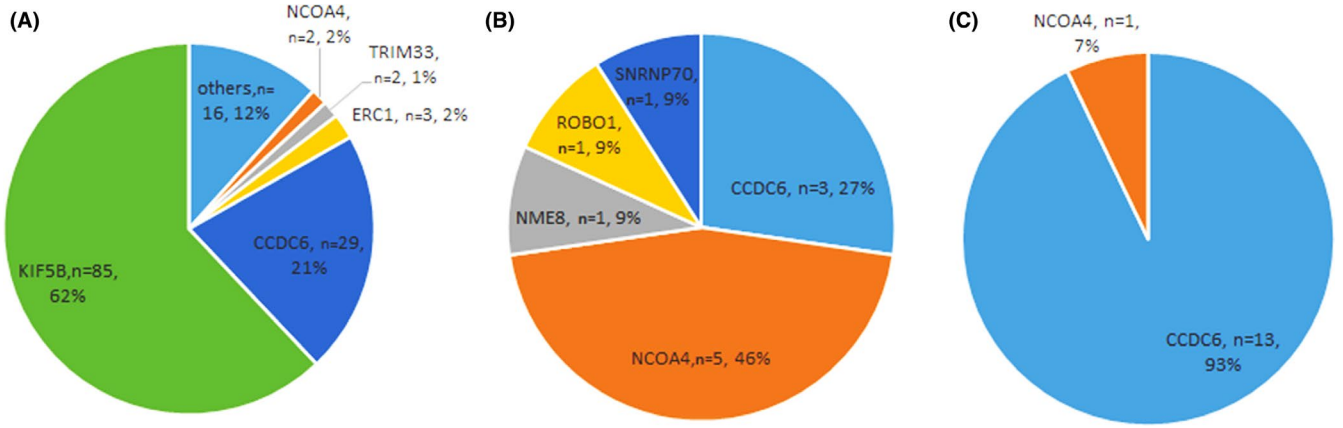


**FIGURE 2** Distribution of fusion partners identified in cancer patients with *RET* fusions. A, In 135 lung cancer patients with *RET* fusions, 137 fusion events were identified with two patients carrying two different *RET* fusions. B, C, Fusion events identified in 11 colorectal cancer patients (B) and 14 papillary thyroid cancer patients (C). Each patient carried only one functional *RET* fusion. Different colors and sizes indicate the frequency of each *RET* fusion partner in all *RET* fusion events identified

**TABLE 2** Patterns of functional *RET* fusions in cancer patients

| Fusion (no.) | Pos1: Pos2 | Counts | Cancer type | Fusion (no.) | Pos1: Pos2 | Counts | Cancer type |
|---|---|---|---|---|---|---|---|
| *KIF5B-RET* (85) | E15: E12 | 63 | LC | *GLI3-RET*[a] | E2: E11 | 1 | LC |
| | E15: E11 | 8 | LC | *GPRC6A-RET*[a] | E1: E12 | 1 | LC |
| | E23: E12 | 4 | LC | *IL1RAPL2-RET*[a] | E2: E12 | 1 | LC |
| | E24: E11 | 3 | LC | *KIAA1598-RET*[a] | E2: E12 | 1 | LC |
| | E24: E9 | 2 | LC | *KIF13A-RET* | E18: E12 | 1 | LC |
| | E24: E10 | 1 | LC | *MALRD1-RET*[a] | E32: E8 | 1 | LC |
| | E16: E12 | 1 | LC | *PRKAR1A-RET* | E2: E10 | 1 | LC |
| | E17: E11 | 1 | LC | *SPECC1-RET*[a] | E4: E12 | 1 | LC |
| | E19: E12 | 1 | LC | *TLN1-RET*[a] | E54: E12 | 1 | LC |
| | E22: E12 | 1 | LC | *TRIM24-RET* | E9: E12 | 1 | LC |
| *CCDC6-RET* (29) | E1: E12 | 28 | LC | *ZNF33B-RET*[a] | E4: E11 | 1 | LC |
| | E2: E12 | 1 | LC | *CCDC6-RET* (3) | E2:E12 | 1 | CRC |
| *ERC1-RET* (3) | E3: E12 | 1 | LC | | E8:E12 | 1 | CRC |
| | E5: E12 | 1 | LC | | E1:E10 | 1 | CRC |
| | E7: E12 | 1 | LC | *NCOA4-RET* (5) | E11:E12 | 4 | CRC |
| *NCOA4-RET* (2) | E10: E12 | 1 | LC | | E9:E12 | 1 | CRC |
| | E8: E12 | 1 | LC | *NME8-RET*[a] | E14:E9 | 1 | CRC |
| *TRIM33-RET* (2) | E16: E10 | 1 | LC | *ROBO1-RET*[a] | E3:E12 | 1 | CRC |
| | E10: E12 | 1 | LC | *SNRNP70-RET*[a] | E2:E12 | 1 | CRC |
| *DNER-RET*[a] | E1: E12 | 1 | LC | *NCOA4-RET* | E8:E12 | 1 | PTC |
| *DPP6-RET*[a] | E2: E12 | 1 | LC | *CCDC6-RET* | E1:E12 | 13 | PTC |
| *EML4-RET* | E17: E12 | 1 | LC | *GABRG3-RET*[a] | E5:E9 | 1 | HCC |
| *FGD5-RET*[a] | E1: E12 | 1 | LC | *OPALIN-RET*[a] | E6:E11 | 1 | GC |
| *GADL1-RET*[a] | E14: E9 | 1 | LC | | | | |

Abbreviations: CRC, colorectal cancer; GC, gastric cancer; HCC, hepatocellular carcinoma; LC, lung cancer; PTC, papillary thyroid cancer.
[a]Novel fusions first reported in this study.

mediate ligand-independent dimerization of the chimeric oncoproteins. They thereby mediate autophosphorylation of the *RET* kinase domain, activating downstream signaling pathways that drive tumor cell proliferation (Figure 4). Of the proteins encoded by the partner genes in this study, 13 (encoded by *EML4*, *CCDC6*, *ERC1*, *KIF13A*, *KIF5B*, *NCOA4*, *TRIM24*, *TRIM33*, *FGD5*, *KIAA1598*, *SNRNP70*, *SPECC1*

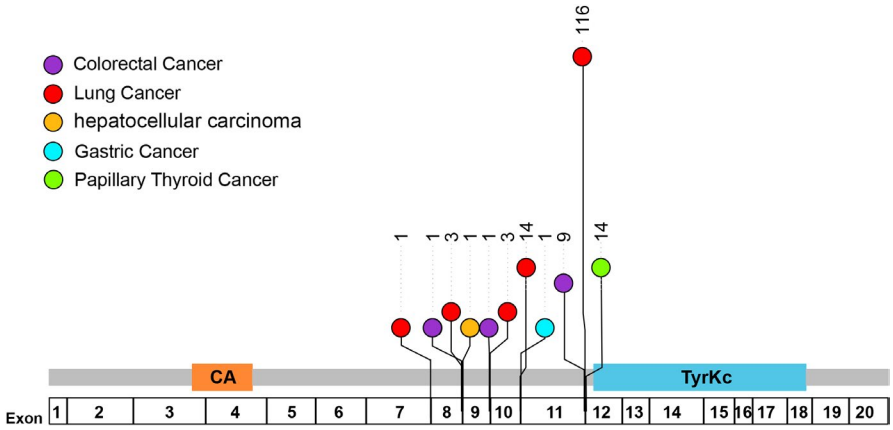


FIGURE 3 Breakpoint positions in *RET*. Different colors represent different cancer types: purple, colorectal cancer; red, lung cancer; orange, hepatocellular carcinoma; cyan, gastric cancer; green, papillary thyroid cancer. Numbers beyond circles represent the counts of functional *RET* fusions detected in different cancer type

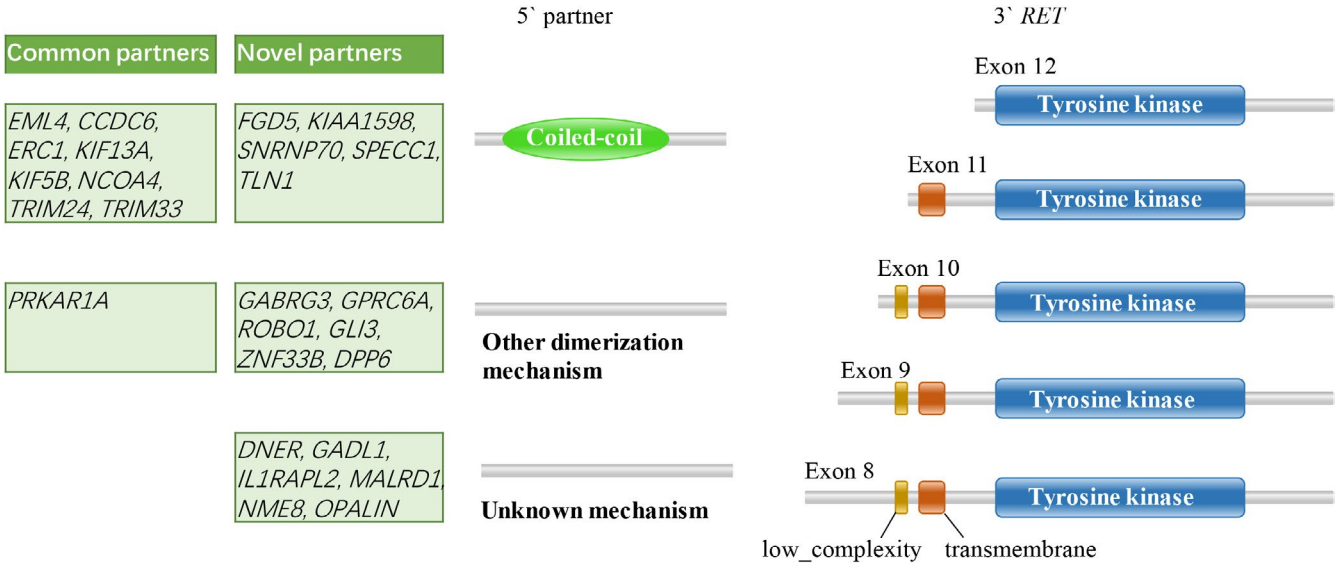


FIGURE 4 Ligand-independent activation of the RET fusion protein. *RET* fusions maintain the tyrosine kinase domain of the 3′ *RET* gene. A variety of fusion partners contribute different domains, such as coiled-coil, to RET fusion proteins. These motifs mediate ligand-independent dimerization of the RET fusion protein. Identification and annotation of genetically mobile domains and analysis of domain architectures (http://smart.embl-heidelberg.de/)

and *TLN1*) have coiled-coil domains that can provide a dimerization motif and seven (encoded by *PRKAR1A*, *GABRG3*, *GPRC6A*, *ROBO1*, *GLI3*, *ZNF33B* and *DPP6*) can form a dimerization through other mechanisms.[51-56] However, there are still six partners (encoded by *DNER*, *GADL1*, *IL1RAPL2*, *MALRD1*, *NME8* and *OPALIN*) that lack the known motifs to form dimerization or oligomerization and need more exploration.

### 3.4 | mRNA features of cases with novel *RET* fusion

Of the 17 novel fusions first reported in this study, five cases were sent for RNA sequencing to verify the breakpoint locations and fusion partners at the transcript level (Table 3). We observed that fusion partners and breakpoints at the transcript level matched those predicted by DNA sequencing in four of the five cases, including *SNRNP70-RET* in CRC and *GABRG3-RET* in HCC. In addition, two LC samples harbored both common and novel *RET* fusions (*KIF5B-RET* and *GLI3-RET*, and *KIF5B-RET* and *MALRD1-RET*), which can be detected by DNA and RNA sequencing. However, *OPALIN-RET* in the GC sample was not detected at the transcript level. The inconsistency between DNA and RNA for fusion detection has been reported recently.[57-59] However, the mechanism of this inconsistency needs more investigation.

At the same time, we analyzed the average per-base coverage for *RET* exons 2-19 in RNA sequencing, which can represent the relative quantity of mRNA transcript for each exon (Figures 5 and S1). Due to the different preferences for each exon when constructing the library, we selected six samples without *RET* fusions as negative controls to observe the distribution of coverage depth. Generally, negative samples had high coverage depth on exons 3, 11, 12 13, and 18, while coverage on exons 4-7 and exons 14-16 were poor (Figures 5 and S1A–F). Two samples with common *RET* fusions (*KIF5B-RET*_E15:E12 and *CCDC6-RET*_E1:E12) were chosen

**TABLE 3** Novel fusion partners of *RET* identified by DNA and RNA next-generation sequencing

| Patient | Gender | Age, y | Cancer type | DNA_fusion | RNA_fusion |
|---|---|---|---|---|---|
| W002899T | Male | 41 | HCC | *GABRG3-RET*_E5:E9 | GABRG3-RET_E5:E9 |
| W027998T | Male | 62 | CRC | *SNRNP70-RET*_E2:E12 | SNRNP70-RET_E2:E12 |
| W001013T | Female | 46 | GC | *OPALIN-RET*_E6:E11 | Negative |
| W016284T | Female | 61 | LC | *KIF5B-RET*_E15:E12 | KIF5B-RET_E15:E12 |
| | | | | *GLI3-RET*_E2:E11 | GLI3-RET_E2:E11 |
| W044019T | Female | 33 | LC | *KIF5B-RET*_E24:E9 | KIF5B-RET_E24:E9 |
| | | | | *MALRD1-RET*_E32:E8 | MALRD1-RET_E32:E8 |

Abbreviations: CRC, colorectal cancer; GC, gastric cancer; HCC, hepatocellular carcinoma; LC, lung cancer.

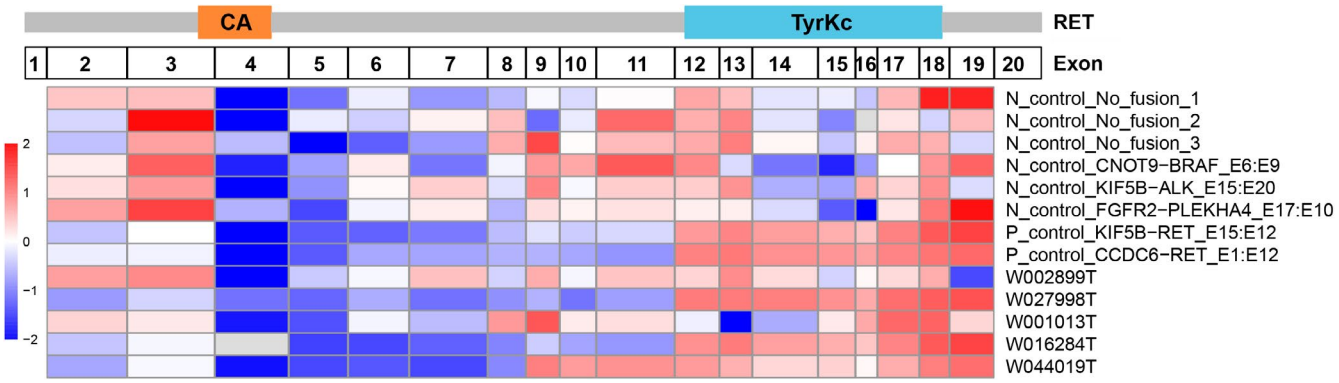


**FIGURE 5** Heatmap of the average per-base coverage for *RET* exons 2-19 (Z-score). Data for each sample was log2-transformed and then Z-score standardized using scale function

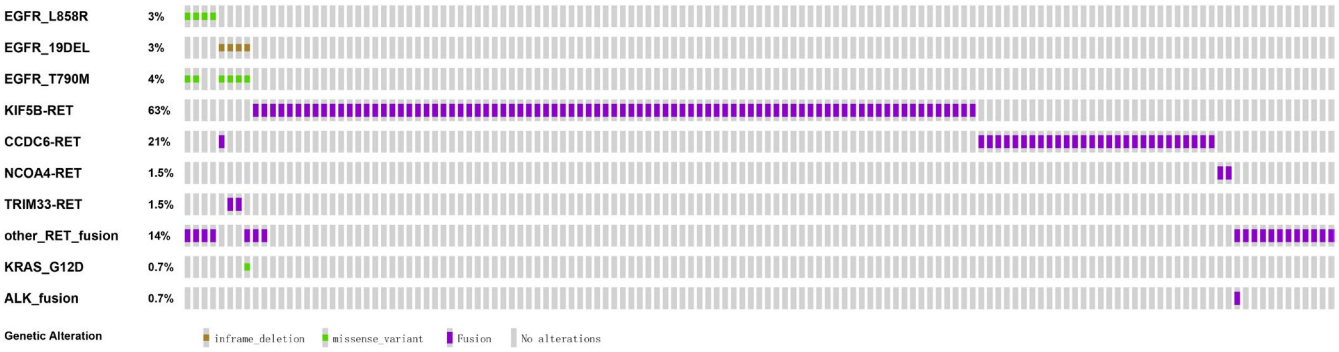


**FIGURE 6** Coexistence status of actionable genes with *RET* fusions in 135 lung cancer patients. Driver mutations EGFR/L858R, EGFR/19DeL, and *ALK* fusion in nine individuals with *RET* fusions were exclusive to each other. The epidermal growth factor receptor (EGFR) tyrosine kinase inhibitor resistance mutation, EGFR T790M, was present in six of eight EGFR-driven patient tumors. The oncoprint of *RET* fusion and other driver mutations was identified using next-generation sequencing. Different colors represent different categories of mutations

as positive controls. The two samples showed low coverage on the exons before the *RET* breakpoint, and there was a sharp rise of the coverage on the exons after the breakpoint (Figures 5 and S1G,H). The *OPALIN-RET* fusion (E6:E11) detected in case W001013T by DNA sequencing was negative in the RNA test, and the distribution of RNA sequencing coverage for each exon was consistent with

**TABLE 4** *RET* fusion and *EGFR* comutation in lung cancer patients

| Sample ID | Age, y/ gender | Sample type | *RET* fusion/AF | *EGFR* mutation/AF | EGFR-TKI history |
|---|---|---|---|---|---|
| W025319T | 36/F | Tissue | *GPRC6A-RET*/0.021 | p.Leu858Arg/0.247 | EGFR-TKI naïve |
| LAL1965T | 61/F | Tissue | *TLN1-RET*/0.071 | p.Leu858Arg/0.598<br>p.Thr790Met/0.228 | Gefitinib, osimertinib |
| LBD9835T | 63/M | Tissue | *TRIM33-RET*/0.064 | p.Glu746_Thr751delinsAla/0.468<br>p.Thr790Met/0.199 | Gefitinib, erlotinib, osimertinib |
| LBE1673NX | 42/F | Plasma | *TRIM33-RET*/0.012 | p.Leu747_Thr751del/0.254<br>p.Thr790Met/0.008 | Erlotinib |
| W054297T | 38/F | Plasma | *KIAA1598-RET*/0.003 | p.Leu858Arg/0.548 | Osimertinib |
| W033932T | 70/F | Plasma | *SPECC1-RET*/0.009 | p.Leu858Arg/0.082<br>p.Thr790Met/0.003 | Gefitinib, osimertinib |
| W045845T | 42/M | Plasma | *TRIM24-RET*/0.052 | p.Glu746_Ala750del/0.169<br>p.Thr790Met/0.048 | Gefitinib, osimertinib |
| W005941N | 26/F | Plasma | *CCDC6-RET*/0.018 | p.Glu746_Ala750del/0.087<br>p.Thr790Met/0.027 | Gefitinib, osimertinib |

Abbreviations: AF, allele frequency; F, female; M, male; TKI, tyrosine kinase inhibitor.

the negative sample (Figures 5 and S1C,I). For the *GABRG3-RET* fusion (E5:E9) in HCC (case W002899T), although the fusion was detected by both DNA and RNA sequencing, there was no transcription enhancement on exons 9-19 (Figures 5 and S1J). A novel *RET* fusion, *SNRNP70-RET* (E2:E12), was confirmed by DNA and RNA sequencing in case W027998T, and the covered depth rose from exon 12 (Figures 5 and S1L). Interestingly, in the other two LC cases (W016284T and W044019T) harboring two different fusions in *RET*, the mRNA level went up from the exon fused with *KIF5B* (exon 12 and exon 9, respectively) rather than the novel partners (exon 11 and exon 8, respectively). This results shows that not all the novel fusions at the DNA level can be detected at the transcript level, and the mRNA levels of these fusion genes might not necessarily increase. The carcinogenic mechanisms of *RET* fused with novel and common partners could be different, which deserves more research and discussion in the future.

### 3.5 | Coexistence of *RET* fusion with other actionable variations in LC patients

Previous studies reported that driver mutations are commonly mutually exclusive.[60,61] However, a coexistence of *RET* fusions with other driver variations was identified in the panel sequencing of lung cancer in this study. In 6.67% (9/135) of LC samples, *RET* fusions coincided with other driver mutations, such as EGFR L858R, EGFR exon 19 deletion, EGFR T790M, KRAS G12D, and/or *EML4-ALK* fusion (Tables S3 and S4, Figure 6).

Notably, seven of the eight patients who harbored *EGFR* driver mutations in *RET* fusion-positive tumors had undergone EGFR-TKI treatment and had developed drug resistance, and six patients developed resistance to first-generation EGFR-TKIs with acquired resistance mutation EGFR T790M (Table 4). Furthermore, *RET* fusions were identified in six patients who had undergone treatment with osimertinib, including one patient (W054297T) who had never received first-generation EGFR-TKIs. Occurrence of *RET* fusion could contribute to resistance to third-generation EGFR-TKIs, as previously reported.[60,61] In addition, *RET* fusions from these eight lung cancer patients with co-occurring *EGFR* driver mutations partnered with rare genes rather than the most frequent (*KIF5B*) in LC. The mechanism behind the "selective" *RET* fusions in contributing to acquired resistance should be explored further. In LC patients with no other well-known driver mutations, the frequency of having a rare fusion partner of *RET* was 16.78% (15/126), lower compared with that in patients with other driver mutations (88.89%, 8/9) ($P < .001$, Pearson's $\chi^2$ test) (Table S3). This finding validates the function of *KIF5B-RET* fusion protein as a driver mutation in LC (Figure 6). In addition, it implies that different fusion partners might have different functions during oncogenesis.

## 4 | DISCUSSION

Cancer-associated *RET* fusions are recognized as *RET* if they occur at the 3′-terminal, thus retaining the complete kinase domain, and can be targeted with recently approved RET inhibitors. *RET* fusion is frequent in PTC, CRC, and LC and can be present in several other cancer types. An accurate detection of *RET* fusion partners and breakpoints is critical for clinical management.

Various molecular testing methods have been developed to detect *RET* fusions, including NGS, RT-PCR, FISH, and IHC. Immunohistochemistry is limited for general application due to its

low sensitivity and specificity.[13,36,37] Reverse transcription-PCR can only detect *RET* fusions with known fusion partners.[29,38,39] Although FISH is highly sensitive, it requires special technical expertise and it is not effective for identification of fusion partners, which could be critical for determining oncogenicity of fusion products.[38,40] The kinase domain of *RET* spans from exon 12 to 18. Breakpoints in *RET* and its fusion partners mainly occur in the intronic regions and can retain the ORF after mRNA splicing. In this study, breakpoints of 3′-terminal *RET* fusion in intron 11 were the most common types, and breakpoints in *RET* introns 7, 8, 9, 10, 12, and 16 were also observed. Breakpoints in the kinase domain of *RET* destroy the activity of the protease, resulting in a nonfunctional fusion product. Therefore, it is necessary to identify the breakpoints of *RET* fusion and other gene fusions. In addition, FISH assay could result in false negative results when fusion partners are in close proximity with *RET* (for instance, *ZNF33B* is ~0.5 Mb away from *RET*), or false positive results when breakpoints are located in the kinase domain (shown as nonfunctional fusions *CCDC60-RET* E2:E17, *SLX4IP-RET* E2:E13, and *UPP2-RET*, E3:E17 in this study). However, it is necessary to clarify the partner genes fused with *RET*, as different fusion partners could activate *RET* through different mechanisms, which means that the sensitivity to inhibitors will also be different. Additionally, *RET* fusion with rare partners could be the cause of resistance to EGFR-TKI. Next-generation sequencing can identify alterations of multiple genes simultaneously with precise identification of fusion partners and breakpoints; therefore, it has become the most widely used procedure in clinical testing.[33]

Co-occurrence of *RET* fusion with other oncogenic driver mutations (eg, *EGFR*, *BRAF*, *ALK*, and *ROS1*) indicates a sensitization or resistance to existing targeted therapies.[27,62-64] Biological functions of these comutations have not been fully explored for effective guidance in clinical therapies. Discrimination between different *RET* fusion types and targeted drug sensitivity is crucial for clinical applications. The function of fusion products with different partners has not been explored. A preference for *KIF5B* (62.04%) in LC, *NCOA4* (45.45%) in CRC, and *CCDC6* (93.33%) in PTC and different fusion partners between acquired TKI resistance and driver mutations in LC reflects different biological functions of fusion products (Figures 2 and 5).

In summary, a series of novel and previously reported *RET* fusions were identified by screening large-scale NGS data from a large sample of Chinese patients with different cancer types. In addition to LC and PTC, the analysis showed that patients with other cancers also occasionally carry *RET* fusions. *RET*-activating fusions, which can be targeted using RET inhibitors, were identified by filtering out those with 5′-terminal *RET* fusions and fusions whose breakpoints occurred in the kinase domain. The findings of this study have potential clinical application as these *RET* fusions can be used to guide cancer diagnosis and/or stratify patients for targeted therapies across different cancer types. Further clinical studies should be undertaken to explore the sensitivity of different fusions in response to RET inhibitors.

## ACKNOWLEDGMENTS

This paper was supported by grants from the Wenzhou Municipal Science and Technology Bureau of China (No. Y20180175). The study was approved by clinical research ethics board of Wenzhou Medical University (No. 2016–197).

## DISCLOSURE

The authors have no conflict of interest.

## ORCID

*Weiran Wang* https://orcid.org/0000-0003-0175-7112

## REFERENCES

1. Takahashi M, Ritz J, Cooper GM. Activation of a novel human transforming gene, ret, by DNA rearrangement. *Cell*. 1985;42:581-588.
2. Alberti L, Carniti C, Miranda C, Roccato E, Pierotti MA. RET and NTRK1 proto-oncogenes in human diseases. *J Cell Physiol*. 2003;195:168-186.
3. McCarty MF. Targeting multiple signaling pathways as a strategy for managing prostate cancer: multifocal signal modulation therapy. *Integr Cancer Ther*. 2004;3:349-380.
4. Gainor JF, Shaw AT. Novel targets in non-small cell lung cancer: ROS1 and RET fusions. *Oncologist*. 2013;18:865-875.
5. Qian YY, Chai S, Liang Z, et al. KIF5B-RET fusion kinase promotes cell growth by multilevel activation of STAT3 in lung cancer. *Mol Cancer*. 2014;13:176.
6. Drilon A, Hu ZI, Lai GGY, Tan DSW. Targeting RET-driven cancers: lessons from evolving preclinical and clinical landscapes. *Nat Rev Clin Oncol*. 2018;15:151-167.
7. Mulligan LM. RET revisited: expanding the oncogenic portfolio. *Nat Rev Cancer*. 2014;14:173-186.
8. Romei C, Ciampi R, Elisei R. A comprehensive overview of the role of the RET proto-oncogene in thyroid carcinoma. *Nat Rev Endocrinol*. 2016;12:192-202.
9. Schram AM, Chang MT, Jonsson P, Drilon A. Fusions in solid tumours: diagnostic strategies, targeted therapy, and acquired resistance. *Nat Rev Clin Oncol*. 2017;14:735-748.
10. Consortium ITP-CAoWG. Pan-cancer analysis of whole genomes. *Nature*. 2020;578:82-93.
11. Bounacer A, Wicker R, Schlumberger M, Sarasin A, Suarez HG. Oncogenic rearrangements of the ret proto-oncogene in thyroid tumors induced after exposure to ionizing radiation. *Biochimie*. 1997;79:619-623.
12. Hamatani K, Eguchi H, Ito R, et al. RET/PTC rearrangements preferentially occurred in papillary thyroid cancer among atomic bomb survivors exposed to high radiation dose. *Cancer Res*. 2008;68:7176-7182.
13. Lipson D, Capelletti M, Yelensky R, et al. Identification of new ALK and RET gene fusions from colorectal and lung cancer biopsies. *Nat Med*. 2012;18:382-384.
14. Kohno T, Tabata J, Nakaoku T. REToma: a cancer subtype with a shared driver oncogene. *Carcinogenesis*. 2020;41:123-129.
15. Kato S, Subbiah V, Marchlik E, Elkin SK, Carter JL, Kurzrock R. RET aberrations in diverse cancers: next-generation sequencing of 4,871 patients. *Clin Cancer Res*. 2017;23:1988-1997.
16. Rich TA, Reckamp KL, Chae YK, et al. Analysis of cell-free DNA from 32,989 advanced cancers reveals novel co-occurring activating RET alterations and oncogenic signaling pathway aberrations. *Clin Cancer Res*. 2019;25:5832-5842.
17. Santoro M, Moccia M, Federico G, Carlomagno F. RET gene fusions in malignancies of the thyroid and other tissues. *Genes*. 2020;11(4):424.

18. Kim P, Jia P, Zhao Z. Kinase impact assessment in the landscape of fusion genes that retain kinase domains: a pan-cancer study. *Brief Bioinform*. 2018;19:450-460.
19. Zhang K, Chen H, Wang Y, et al. Clinical characteristics and molecular patterns of RET-rearranged lung cancer in Chinese patients. *Oncol Res*. 2019;27:575-582.
20. Yakushina VD, Lerner LV, Lavrov AV. Gene fusions in thyroid cancer. *Thyroid*. 2018;28:158-167.
21. Li AY, McCusker MG, Russo A, et al. RET fusions in solid tumors. *Cancer Treat Rev*. 2019;81:101911.
22. Saito M, Shimada Y, Shiraishi K, et al. Development of lung adenocarcinomas with exclusive dependence on oncogene fusions. *Cancer Res*. 2015;75:2264-2271.
23. Hamatani K, Eguchi H, Koyama K, Mukai M, Nakachi K, Kusunoki Y. A novel RET rearrangement (ACBD5/RET) by pericentric inversion, inv(10)(p12.1;q11.2), in papillary thyroid cancer from an atomic bomb survivor exposed to high-dose radiation. *Oncol Rep*. 2014;32:1809-1814.
24. Iyama K, Matsuse M, Mitsutake N, et al. Identification of three novel fusion oncogenes, SQSTM1/NTRK3, AFAP1L2/RET, and PPFIBP2/RET, in thyroid cancers of young patients in Fukushima. *Thyroid*. 2017;27:811-818.
25. Cancer Genome Atlas Research N. Integrated genomic characterization of papillary thyroid carcinoma. *Cell*. 2014;159:676-690.
26. Staubitz JI, Musholt TJ, Schad A, et al. ANKRD26-RET – a novel gene fusion involving RET in papillary thyroid carcinoma. *Cancer Genet*. 2019;238:10-17.
27. Xu H, Shen J, Xiang J, et al. Characterization of acquired receptor tyrosine-kinase fusions as mechanisms of resistance to EGFR tyrosine-kinase inhibitors. *Cancer Manag Res*. 2019;11:6343-6351.
28. Lira ME, Choi Y-L, Lim SM, et al. A single-tube multiplexed assay for detecting ALK, ROS1, and RET fusions in lung cancer. *J Mol Diagn*. 2014;16:229-243.
29. Gautschi O, Milia J, Filleron T, et al. Targeting RET in patients with RET-rearranged lung cancers: results from the global, multicenter RET registry. *J Clin Oncol*. 2017;35:1403-1410.
30. Paratala BS, Chung JH, Williams CB, et al. RET rearrangements are actionable alterations in breast cancer. *Nat Commun*. 2018;9:4821.
31. Pietrantonio F, Di Nicolantonio F, Schrock AB, et al. RET fusions in a small subset of advanced colorectal cancers at risk of being neglected. *Ann Oncol*. 2018;29:1394-1401.
32. Selpercatinib MA. First approval. *Drugs*. 2020;80:1119-1124.
33. Stinchcombe TE. Current management of RET rearranged non-small cell lung cancer. *Ther Adv Med Oncol*. 2020;12:1758835920928634.
34. Subbiah V, Velcheti V, Tuch BB, et al. Selective RET kinase inhibition for patients with RET-altered cancers. *Ann Oncol*. 2018;29:1869-1876.
35. Subbiah V, Gainor JF, Rahal R, et al. Precision targeted therapy with BLU-667 for RET-driven cancers. *Cancer Discov*. 2018;8:836-849.
36. Ferrara R, Auger N, Auclin E, Besse B. Clinical and translational implications of RET rearrangements in non-small cell lung cancer. *J Thorac Oncol*. 2018;13:27-45.
37. Go H, Jung YJ, Kang HW, et al. Diagnostic method for the detection of KIF5B-RET transformation in lung adenocarcinoma. *Lung Cancer*. 2013;82:44-50.
38. Wang R, Hu H, Pan Y, et al. RET fusions define a unique molecular and clinicopathologic subtype of non-small-cell lung cancer. *J Clin Oncol*. 2012;30:4352-4359.
39. Pan Y, Zhang Y, Li Y, et al. ALK, ROS1 and RET fusions in 1139 lung adenocarcinomas: a comprehensive study of common and fusion pattern-specific clinicopathologic, histologic and cytologic features. *Lung Cancer*. 2014;84:121-126.
40. Tsuta K, Kohno T, Yoshida A, et al. RET-rearranged non-small-cell lung carcinoma: a clinicopathological and molecular analysis. *Br J Cancer*. 2014;110:1571-1578.
41. Li H, Durbin R. Fast and accurate short read alignment with Burrows-Wheeler transform. *Bioinformatics*. 2009;25:1754-1760.
42. Cibulskis K, Lawrence MS, Carter SL, et al. Sensitive detection of somatic point mutations in impure and heterogeneous cancer samples. *Nat Biotechnol*. 2013;31:213-219.
43. Saunders CT, Wong WS, Swamy S, Becq J, Murray LJ, Cheetham RK. Strelka: accurate somatic small-variant calling from sequenced tumor-normal sample pairs. *Bioinformatics*. 2012;28:1811-1817.
44. Chen S, Liu M, Huang T, Liao W, Xu M, Gu J. GeneFuse: detection and visualization of target gene fusions from DNA sequencing data. *Int J Biol Sci*. 2018;14:843-848.
45. Cancer Genome Atlas Research N. Comprehensive molecular profiling of lung adenocarcinoma. *Nature*. 2014;511:543-550.
46. Kim D, Langmead B, Salzberg SL. HISAT: a fast spliced aligner with low memory requirements. *Nat Methods*. 2015;12:357-360.
47. Ge H, Liu K, Juan T, Fang F, Newman M, Hoeck W. FusionMap: detecting fusion genes from next-generation sequencing data at base-pair resolution. *Bioinformatics*. 2011;27:1922-1928.
48. Pierotti MA, Santoro M, Jenkins RB, et al. Characterization of an inversion on the long arm of chromosome 10 juxtaposing D10S170 and RET and creating the oncogenic sequence RET/PTC. *Proc Natl Acad Sci USA*. 1992;89:1616-1620.
49. Attie-Bitach T, Abitbol M, Gerard M, et al. Expression of the RET proto-oncogene in human embryos. *Am J Med Genet*. 1998;80:481-486.
50. Ju YS, Lee W-C, Shin J-Y, et al. A transforming KIF5B and RET gene fusion in lung adenocarcinoma revealed from whole-genome and transcriptome sequencing. *Genome Res*. 2012;22:436-445.
51. Norskov-Lauritsen L, Jorgensen S, Brauner-Osborne H. N-glycosylation and disulfide bonding affects GPRC6A receptor expression, function, and dimerization. *FEBS Lett*. 2015;589:588-597.
52. Aleksandrova N, Gutsche I, Kandiah E, et al. Robo1 forms a compact dimer-of-dimers assembly. *Structure*. 2018;26(2):320-328 e4.
53. Krishna SS, Majumdar I, Grishin NV. Structural classification of zinc fingers: survey and summary. *Nucleic Acids Res*. 2003;31:532-550.
54. Bezerra GA, Dobrovetsky E, Seitova A, Fedosyuk S, Dhe-Paganon S, Gruber K. Structure of human dipeptidyl peptidase 10 (DPPY): a modulator of neuronal Kv4 channels. *Sci Rep*. 2015;5:8769.
55. Drilon A, Hu ZI, Lai GGY, Tan DSW. Targeting RET-driven cancers: lessons from evolving preclinical and clinical landscapes. *Nat Rev Clin Oncol*. 2018;15:150.
56. Luscher B, Fuchs T, Kilpatrick CL. GABAA receptor trafficking-mediated plasticity of inhibitory synapses. *Neuron*. 2011;70:385-409.
57. Li W, Guo L, Liu Y, et al. Potential unreliability of uncommon ALK, ROS1, and RET genomic breakpoints in predicting the efficacy of targeted therapy in NSCLC. *J Thorac Oncol*. 2021;16:404-418.
58. Cui M, Han Y, Li P, et al. Molecular and clinicopathological characteristics of ROS1-rearranged non-small-cell lung cancers identified by next-generation sequencing. *Mol Oncol*. 2020;14:2787-2795.
59. Davies KD, Le AT, Sheren J, et al. Comparison of molecular testing modalities for detection of ROS1 rearrangements in a cohort of positive patient samples. *J Thorac Oncol*. 2018;13:1474-1482.
60. Shaw AT, Yeap BY, Mino-Kenudson M, et al. Clinical features and outcome of patients with non-small-cell lung cancer who harbor EML4-ALK. *J Clin Oncol*. 2009;27:4247-4253.
61. Horn L, Pao W. EML4-ALK: honing in on a new target in non-small-cell lung cancer. *J Clin Oncol*. 2009;27:4232-4235.
62. Klempner SJ, Bazhenova LA, Braiteh FS, et al. Emergence of RET rearrangement co-existing with activated EGFR mutation in EGFR-mutated NSCLC patients who had progressed on first- or second-generation EGFR TKI. *Lung Cancer*. 2015;89:357-359.
63. Offin M, Somwar R, Rekhtman N, et al. Acquired ALK and RET gene fusions as mechanisms of resistance to osimertinib in EGFR-mutant lung cancers. *JCO Precis Oncol*. 2018;2.

64. Piotrowska Z, Isozaki H, Lennerz JK, et al. Landscape of acquired resistance to osimertinib in EGFR-mutant NSCLC and clinical validation of combined EGFR and RET inhibition with osimertinib and BLU-667 for acquired RET fusion. *Cancer Discov*. 2018;8:1529-1539.

## SUPPORTING INFORMATION

Additional supporting information may be found in the online version of the article at the publisher's website.

**How to cite this article:** Shi M, Wang W, Zhang J, et al. Identification of *RET* fusions in a Chinese multicancer retrospective analysis by next-generation sequencing. *Cancer Sci*. 2022;113:308–318. https://doi.org/10.1111/cas.15181